J Solid State Electrochem (2008) 12:193–201
DOI 10.1007/s10008-007-0380-7

ORIGINAL PAPER

Effect of chemical structure of hydroxyethyl imidazolines inhibitors on the CO_2 corrosion in water–oil mixtures

W. Villamizar · M. Casales · L. Martinez · J. G. Chacon-Naca · J. G. Gonzalez-Rodriguez

Received: 5 March 2007 / Revised: 17 April 2007 / Accepted: 14 June 2007 / Published online: 26 July 2007

Abstract The corrosion inhibition of oleic, coconut, and stearic acid modified hydroxyethyl imidazolines on 1018 carbon steel was evaluated by using potenthiodynamic polarization curves, linear polarization resistance, and electrochemical impedance spectroscopy techniques. Solutions included deaerated CO_2 saturated 3% NaCl with and without Diesel at 50 °C. Regardless of the presence of diesel, the corrosion rate was decreased with the addition of the inhibitors, but the time to reach a steady state was longer than when the oily part, i.e., diesel, was present. This was because the inhibitors are oil soluble, and with diesel, they are more easily transported towards the metal surface. With diesel, the formed film seems to be more stable and protective, not allowing the electrolyte to corrode the sample increasing the efficiency values up to 87 and 94%. The most efficient inhibitors were the coconut type fatty acid hidroxyethyl imidazoline because the formed film was much more stable from the beginning of the test, whereas the least efficient was the stearic acid modified hydroxyethyl imidazoline.

W. Villamizar · M. Casales · L. Martinez
Instituto de Ciencias Físicas,
Universidad Nacional Autonoma de México,
Av. Universidad S/N, Col. Chamilpa,
62210 Cuernavaca Mor, Mexico

J. G. Chacon-Naca
CIMAV-Complejo Industrial Chihuahua,
Miguel de Cervantes 108,
Chihuahua, Mexico

J. G. Gonzalez-Rodriguez (✉)
UAEM-CIICAp,
Av. Universidad 1001, Col. Chamilpa,
62210 Cuernavaca, Mor, Mexico
e-mail: ggonzalez@uaem.mx

Keywords CO_2 corrosion · Hydroxyethyl imidazolines · Electrochemical techniques

Introduction

Oilfield corrosion manifests itself in several forms, among which CO_2 corrosion (sweet corrosion) and hydrogen sulfide (H_2S) corrosion (sour corrosion) in the produced fluids and corrosion by oxygen dissolved in water injection are by far the most prevalent forms of attack [1].

The injection of corrosion inhibitor is a standard practice in oil and gas production systems to control internal corrosion of carbon steel structures. Nitrogen-based organic inhibitors, such as imidazolines or their salts have been successfully used in these applications even without an understanding of the inhibition mechanism [2–4]. The corrosion inhibition of organic compounds is related to their adsorption properties. Adsorption depends on the nature and the state of the metal surface, the type of corrosive environment, and the chemical structure of the inhibitor [5]. Studies report that the adsorption of the organic inhibitors mainly depends on some physicochemical properties of the molecule, related to its functional groups, to the possible steric effects and electronic density of donor atoms. Adsorption is supposed to depend on the possible interaction of the π-orbitals of the inhibitor with the d-orbitals of the surface atoms, which induce greater adsorption of the inhibitor molecules onto the surface of metal, leading to the formation of a corrosion protection film [6].

Different derivatives from imidazolines are employed as corrosion inhibitors. Particularly, hydroxyethyl-imidazolines have been found to be highly efficient for this purpose [7]. This type of imidazolines has a general structure as

given on Fig. 1, where *R* is an alkyl chain derivative, and HO is the hydroxyethyl group. The alkyl group can change, and therefore, affect the inhibitor properties. Normally, it is believed that inhibitors in crude oil are adsorbed on the metal surface forming a hydrophobic film because oils contain some dissolved water, responsible, among other factors, of the corrosion. Even though they have been specially employed in the oil industry, only recently, a respectable amount of studies have been undertaken to understand how they work [2, 8–14]. These works imply some key questions regarding the structure–performance relationships of imidazolines, the role of the oily phase and the hydrocarbon chain head group and pendant group in film formation, the thickness of the imidazoline film, the stability of the imidazoline group and the solution composition and hydrolysis of imidazoline, among others.

The purpose of this paper is to evaluate the role of the alkyl group on the behavior of hydroxyethyl imidazolines as corrosion inhibitors in the CO_2 corrosion of 1018 carbon steel using electrochemical technique in an environment containing NaCl and CO_2. To see the effect of the oily part, 10% of diesel was added to simulate environments found in the transport of crude oil and gives a solution with an acceptable conductivity value as suggested by Quiroga-Becerra [15].

Experimental

Test material

Cylindrical electrode 4.55 cm in length, 0.63 cm in diameter, fabricated from 1018 type carbon steel, with an exposed area of 1.0 cm^2 were used as working electrode. Before testing, the electrode was polished to 600 grit SIC emery paper and then cleaned with alcohol, acetone, and distilled water.

Test solution

Three types of commercial hydroxyethyl imidazolines were used in this study with a general structure as shown in Fig. 1. The first hydroxyethyl imidazoline (1H-imidazole-ethanol,4,5-dihydro,-2-C15-17 unsaturated alkyl derivatives, HEI-18I, with C_{17} as alkyl group) is a high molecular weight substituted imidazoline, based on an oleic-type fatty acid; the second hydroxyethyl imidazoline (1H-imidazole-ethanol,4,5-dihydro,-2-nor coco alkyl derivatives, HEI-12 and C_{12} as alkyl group) is an oil dispersable imidazoline, based on a coconut type fatty acid; finally, the third hydroxyethyl imidazoline (1H-imidazole-ethanol,2-Heptadecyl-4,5-Dihydro, HEI-18, and C_{17} as alkyl group) is high molecular weight, stearic acid substituted imidazoline. The inhibitors were dissolved in pure 2-propanol. The concentration of the inhibitor used in this work was 20 ppm and the temperature kept at 50 °C. The testing solution consisted of either pure 3% NaCl solution or 90% of this solution + 10% Diesel emulsion, heated, deaerated with nitrogen gas, CO_2 saturated for 2 hours, and then the inhibitor was added. Continuous stirring was used, and CO_2 bubbled during the tests. The used cell is the one given by standard ASTM G5 [16] and shown on Fig. 2.

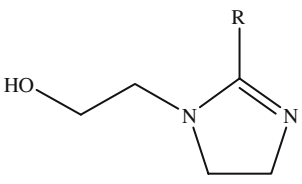

Fig. 1 Scheme showing the general structure of the different hydroxyethyl imidazolines, where R is an Alkyl chain derivative and OH is the hydroxyethyl group

Electrochemical measurements

Electrochemical techniques employed included potentiodynamic polarization curves, linear polarization resistance, LPR, and electrochemical impedance spectroscopy, EIS, measurements. Polarization curves were recorded at a constant sweep rate of 1 mV/s, and the scanning range was from −300 to +300 mV with respect to the open circuit potential, E_{corr}. Measurements were obtained by using a conventional three-electrodes glass cell with two graphite rods as counter electrodes symmetrically distributed and a saturated calomel electrode (SCE) as reference with a Lugging capillary bridge. Inhibition efficiencies (*E(%)*)

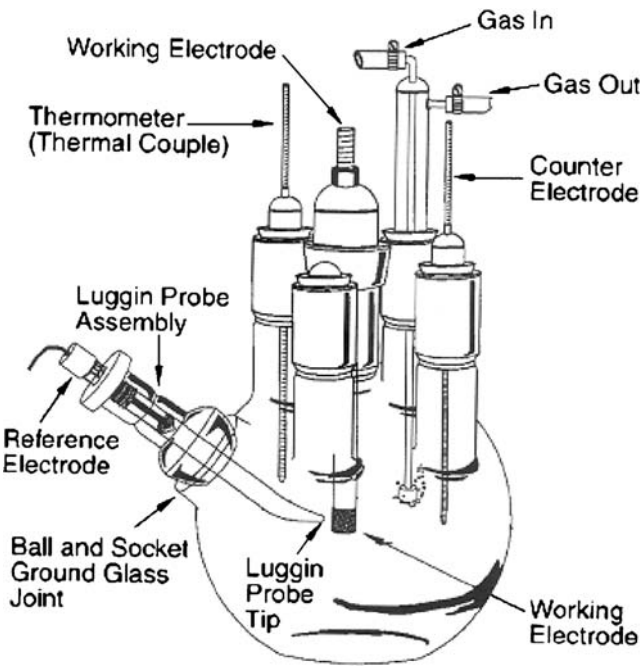

Fig. 2 Scheme showing the experimental set-up for electrochemical measurements

were determined from the corrosion current densities calculated by the Tafel extrapolation method according to the following equation

$$E(\%) = \left[\frac{i_b - i_i}{i_b}\right] \times 100 \quad (1)$$

where i_b is the corrosion rate without inhibitor and i_i the corrosion rate in the solution with inhibitor. Tests were started 30 min after inhibitor was added.

LPR measurements were carried out by polarizing the specimen from +10 to −10 mV with respect to E_{corr}, at a scanning rate of 1 mV/s. Inhibition efficiencies [E(%)] were determined according to the following equation

$$E(\%) = \frac{R_{p,i} - R_{p,b}}{R_{p,i}} \times 100 \quad (2)$$

where $R_{p,b}$ is the linear polarization resistance without inhibitor, and $R_{p,i}$ is the linear polarization resistance with inhibitor. Tests were started once the solution was deaerated and saturated with CO_2, and only 30 min after inhibitor was added, taking readings every 20 min during 9 h.

Electrochemical impedance spectroscopy tests were carried out at E_{corr} by using a signal with an amplitude of 10 mV and a frequency interval of 0.1–100 kHz.. An AUTO DC ACM potentiostat controlled by a desktop computer was used for the LPR tests and polarization curves, whereas for the EIS measurements, a model PC4 300 Gamry potentiostat was used. All the tests were carried out at 50 °C and lasted for 9 h and started 30 min after addition of the inhibitor, taking readings every hour. For each electrochemical test, i.e. polarization curves, LPR or EIS readings, a fresh solution was used.

Results and discussion

Polarization curves

Figures 3 and 4 show the polarization curves for carbon steel in CO_2 saturated 3% NaCl and 3% NaCl + diesel solutions with the addition of 20 ppm of inhibitors, respectively. These curves show that both the cathodic and anodic current densities were lowered by the addition of the imidazolines in the presence of diesel, i.e., the oily part. On the other hand, in the absence of this oily part, only the anodic current density values were lowered with the addition of the inhibitors. No significant changes among the three inhibitors is observed: the values for both the free corrosion potential, E_{corr}, and the corrosion current density, i_{corr}, were virtually the same, see Table 1. In all cases, the E_{corr} values for the inhibited solutions were less active than that for the blank solution for around 100 mV. The highest efficiency, around 63%, was obtained with inhibitors HEI-12 and HEI-18I. However, when diesel is added, the E_{corr} value of the blank solution and the inhibited solutions was practically the same, around −720 mV, except for inhibitor HEI-12, with an E_{corr} value slightly more active than all the other solutions, even than the blank solution, −750 mV. Nevertheless, in this case, the efficiency values increased, reaching a highest value, around 93%, again with inhibitors HEI-12 and HEI-18I, as can be seen on Table 2. This behavior can be explained because inhibitor HEI-18I contains 17 C and is oil soluble, HEI-18 contains 17 C in the chain but is soluble only if heated, and HEI-12 has 12 C in the chain and is oil dispersable. None of the inhibitors is water-soluble, so, when the oily phase is present, the inhibitors' solubility increase, and they are more easily

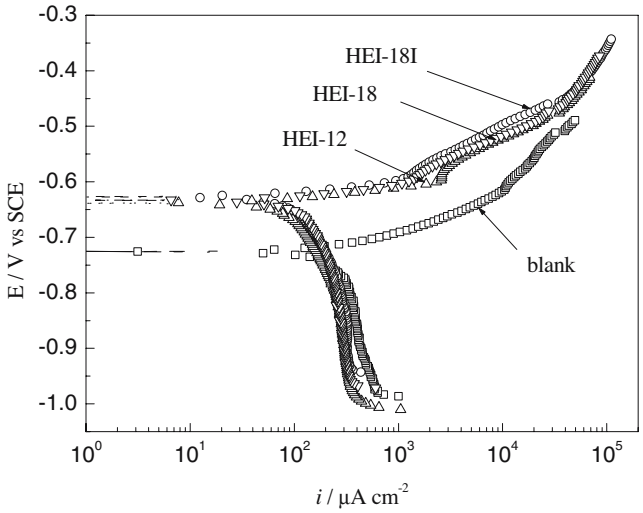

Fig. 3 Polarization curves for carbon steel with the different imidazolines in 3% NaCl solution

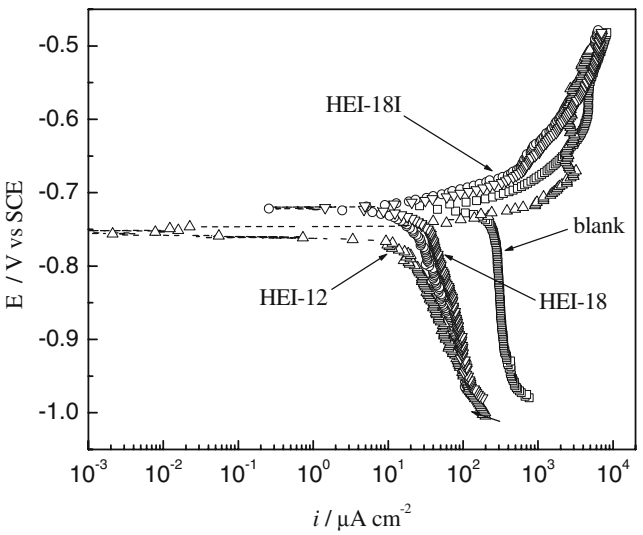

Fig. 4 Polarization curves for 1018 carbon steel with different imidazolines in the 3% NaCl + diesel with CO_2

transported towards the surface to be adsorbed to form a film against corrosion.

No linear Tafel region appeared on the cathodic branch, so the reported I_{corr} values on Table 1 are approximated ones calculated by extrapolating the anodic Tafel slope to the free corrosion potential [17]. In any case, the difference between the corrosion current density values for the inhibited and the uninhibited solutions, one order of magnitude, especially in the presence of diesel, justify the Tafel extrapolation. On the cathodic side, on the other hand, only a diffusion-limiting current density was observed, and this justifies the used extrapolation method suggested in Thompson and Payer [17], which indicated that the different imidazolines could be adsorbed on the metal surface without applying any potential on the electrode. This cathodic limit current can be due to a decrease on the H^+ ion concentration near the metallic surface and to a slow hydration of the CO_2.

Electrochemical parameters, corrosion rate, and efficiency values for the three imidazolines with and without diesel are shown in Tables 1 and 2, respectively. It can be seen that the free corrosion potential value, E_{corr}, was unaltered for the blank when diesel is added; however, this value is made more cathodic for the three imidazolines when diesel is present. Similarly, the corrosion current density value, i_{corr} , for the blank solution was unaltered with the addition of diesel, but this value was lowered for the different imidazolines for almost one order of magnitude. The efficiency values for the different imidazolines was always lower in the absence of diesel than when this is added, as in the former, this value was close to 90%, whereas in the latter, it was between 55 and 65%. In both cases, the highest efficiency was obtained with imidazoline HEI-12, and the lowest value was for imidazoline HEI-18.

LPR results

The change in the linear polarization resistance values, R_p, for the 3% NaCl and 3% NaCl + diesel solutions with and without the addition of the different inhibitors are given in Fig. 5. These tests lasted for 24 h, and as the R_p values remained constant, we present here the data for the first 2 h only. Before the addition of the inhibitors, the R_p values were slightly higher without diesel except for the HEI-18 type inhibitor. When the inhibitors were added, the R_p values for the solution with diesel increased up to four orders of magnitude with respect to the uninhibited solution, except for inhibitor HEI-18I, where this increase was slightly higher than one order of magnitude. On the other hand, for the solution without diesel, the R_p values increased only two orders of magnitude with the addition of inhibitor HEI-18I, whereas for inhibitors HEI-12 and HEI-18, the increase in the R_p value was much lower than one order of magnitude. The variation in R_p values is ascribed to the different solubility and their hydrophobic character of the imidazolines in the two environments. In fact, the three inhibitors are insoluble in water and very hydrophobic; however, inhibitor HEI-18I is oil soluble, HEI-18 is soluble only if heated, as in this case, and the imidazoline and inhibitor HEI-12 is oil dispersable. When only water is present, due to their lack of solubility in water, they cannot be so easily transported towards the surface, but when diesel, the oily part, is present, their solubility increase, and they can be more easily transported towards the metal surface. As HEI-12 has only 12 C atoms in the chain of its alkyl group, its transport towards the metal is easier than both HEI-18I and HEI-18, which have 17 C atoms in the chain of their alkyl groups.

Table 1 Electrochemical parameters for 1018 carbon steel in NaCl 3% saturated with CO_2 and the different types of imidazolines

Inhibitor	E_{corr} (V)	i_{corr} (μA cm^{-2})	b_a (mV/decade)	E (%)
Blank	−0.730±0.004	273.9±64.7	63.6±2.3	
HEI-18I	−0.636±0.007	103.8±32.9	52.7±7.5	62.2
HEI-12	−0.643±0.005	98.8±23.14	42.7±9.3	63.9
HEI-18	−0.638±0.004	123.6±3.8	53.5±0.95	54.9

Table 2 Electrochemical parameters for 1018 carbon steel in NaCl 3% + diesel saturated with CO_2 and the different types of imidazolines

Inhibitor	E_{corr} (V)	i_{corr} (μA cm^{-2})	b_a (mV/decade)	E (%)
Blank	−0.720±0.006	258.5±33.8	82.7±15.9	
HEI-18I	−0.721±0.007	21.2±1.6	65.4±16.0	91.8
HEI-12	−0.751±0.006	14.7±1.6	54.9±17.2	94.3
HEI-18	−0.722±0.008	33.0±3.1	70.9±21.7	87.2

EIS results for uninhibited solutions

The Nyquist data for the uninhibited 3% NaCl without and with diesel are given in Fig. 6. This behavior is typical for solid metal electrodes that show frequency dispersion of the impedance data [18]. Electrically equivalent circuits are generally used to model the electrochemical behavior and calculate the parameters of interest such as electrolyte resistance (R_s), charge transfer resistance (R_{ct}) and double layer capacitance (C_{dl}) [19]. When a non-ideal frequency response is present, it is commonly accepted to employ distributed circuit elements in an equivalent circuit. The most widely used is constant phase element (CPE), for better fit quality, a general expression for many circuits,

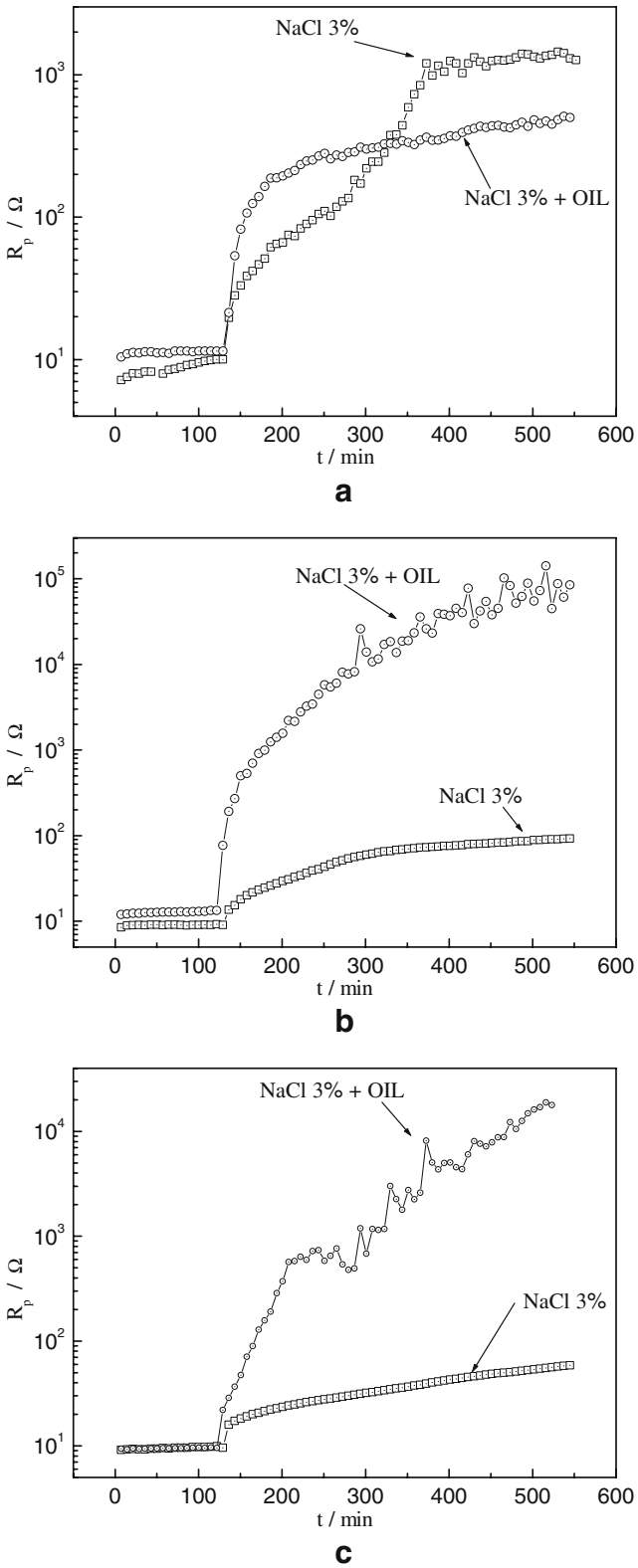

Fig. 5 Change of the linear polarization resistance (R_p) with time for 3% NaCl and 3% NaCl + diesel solution with the different types of imidazolines. **a** HEI-18I; **b** HEI-12; **c** HEI-18

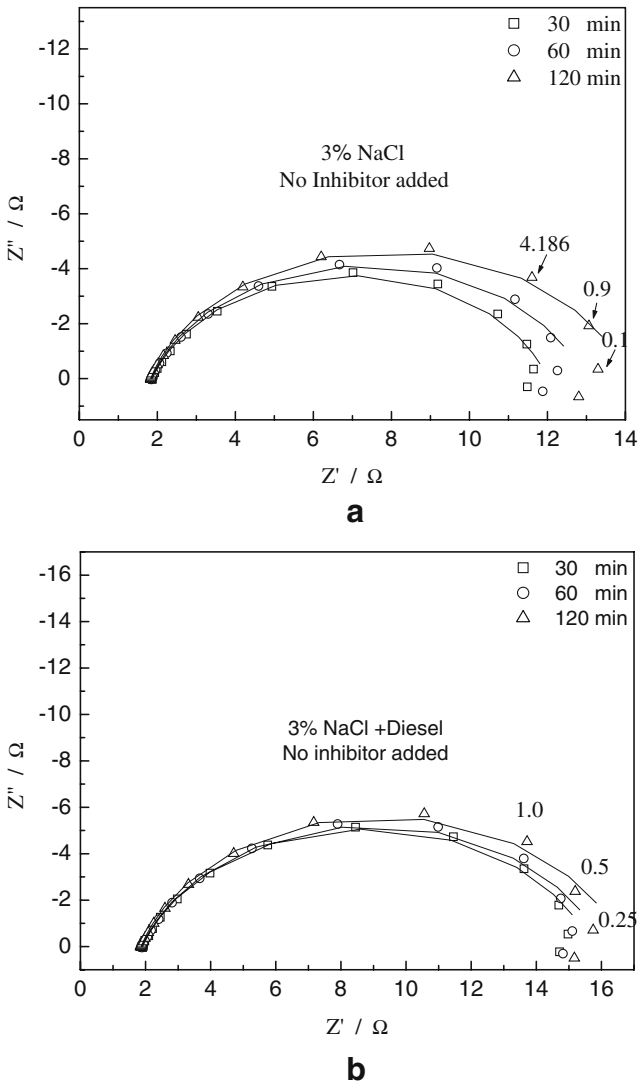

Fig. 6 Nyquiat diagrams for uninhibited **a** 3% NaCl and **b** 3% NaCl + diesel solutions. *Symbols* represent experimental values; *solid lines* are the predicted values. *Numbers inside* indicate frequencies, in Hz

which has a noninteger power dependence on the frequency. The impedance of a CPE is described by the expression:

$$Z_{\mathrm{CPE}} = Y^{-1}(iw)^n \tag{3}$$

where Y is a proportional factor, i is $\sqrt{-1}$, w is $2\pi f$, f is the frequency, and n has the meaning of a phase shift [20]. Often, a CPE is used in a model in place of a capacitor to compensate for non-homogeneity in the system to take into

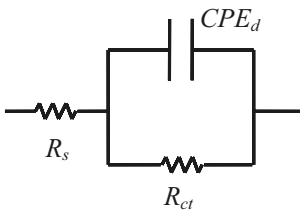

Fig. 7 Equivalent circuit used to represent the impedance results for uninhibited 3% NaCl and 3% NaCl + diesel solutions

Table 3 Circuit parameters for 1018 carbon steel in uninhibited 3% NaCl solution

t (min)	R_s (Ω)	CPE_d		R_{ct} (Ω)
		Y_0 (Ω^{-1} s^n) $\times 10^{-3}$	n	
30	0.58	4.26	0.798	10.45
60	0.58	4.30	0.814	11.07
120	0.59	4.81	0.815	12.56

account irregularities of the surface such as roughness or because properties such as double layer capacitance, charge transfer rate, etc...are nonuniformly distributed. For an ideal capacitor, Y is $1/C$ and $n=1$, whereas for a nonideal capacitor $n<1$, and the semicircle in the $Z_{re}-Z_{im}$ spectra is more and more depressed.

The impedance spectra for both solutions exhibited in all cases a single (capacitive like) semicircle and then only one constant phase element, which can be modeled as an electric equivalent circuit given in Fig. 7. The fitting parameters for both solutions are given in Tables 3 and 4, respectively, and they appear as solid lines on Fig. 6. The R_{ct} values when diesel is present are slightly higher than when diesel is absent, indicating that the oily part, without inhibitor, does not form a protective film. The increase in the proportional factor Y of CPE has been related to the growing area of an iron carbonate deposit on the surface of the samples. At 50 °C, our testing temperature, iron carbonate film starts to be adherent, protective, and nonconductive, and reduces the corrosion rate by forming a barrier, protective or not. After 24 h of testing, the specimen was completely covered by corrosion products which came off very easily, indicating that they were not protective.

EIS results for inhibited solutions

Nyquist impedance spectra, for the 3% NaCl solution without diesel, after addition of the three inhibitors at different exposure times, are shown in Fig. 8a–c, respectively. All experimental spectra have a depressed semicircular shape in the complex impedance plane, with the center under the real axis. The magnitude of the impedance increases continuously with time for all inhibitors, but this

Table 4 Circuit parameters for 1018 carbon steel in uninhibited 3% NaCl + diesel solution

t (min)	R_s (Ω)	CPE_d		R_{ct} (Ω)
		Y_0 (Ω^{-1} s^n) $\times 10^{-3}$	n	
30	1.91	3.35	0.801	13.98
60	1.88	3.74	0.800	14.45
120	1.86	3.99	0.816	15.11

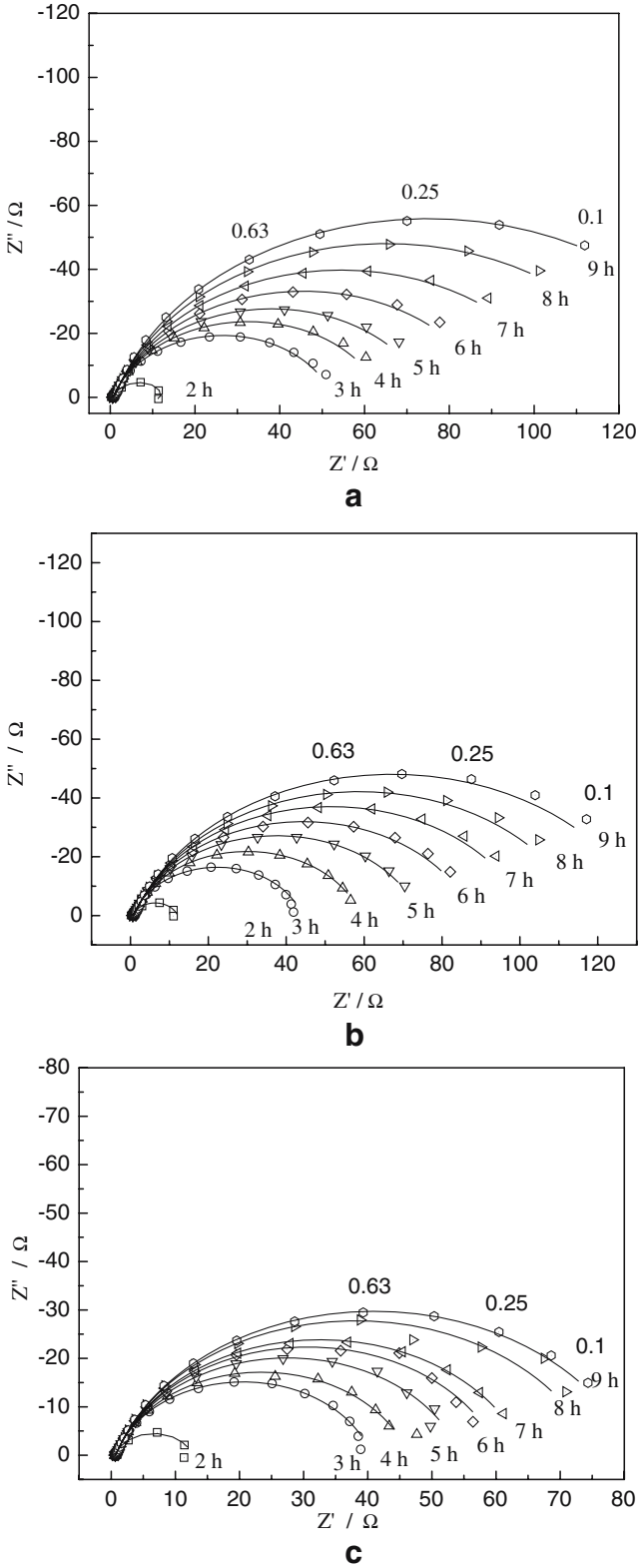

Fig. 8 Nyquist diagrams for 1018 carbon steel in 3% NaCl solution with the different imidazolines. **a** HEI-18I; **b** HEI-12; **c** HEI-18

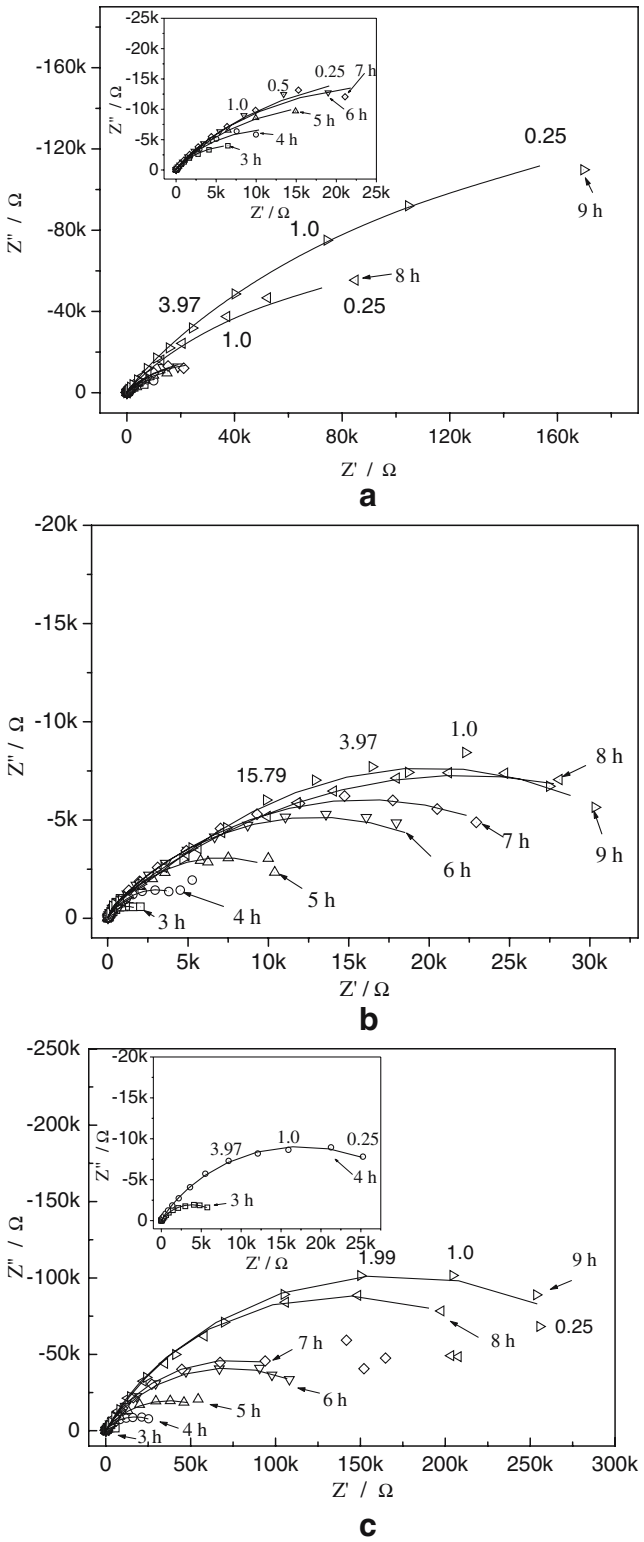

Fig. 9 Nyquist diagrams for 1018 carbon steel in the 3% NaCl + diesel solution with the different imidazolines. **a** HEI-18I; **b** HEI-12; **c** HEI-18

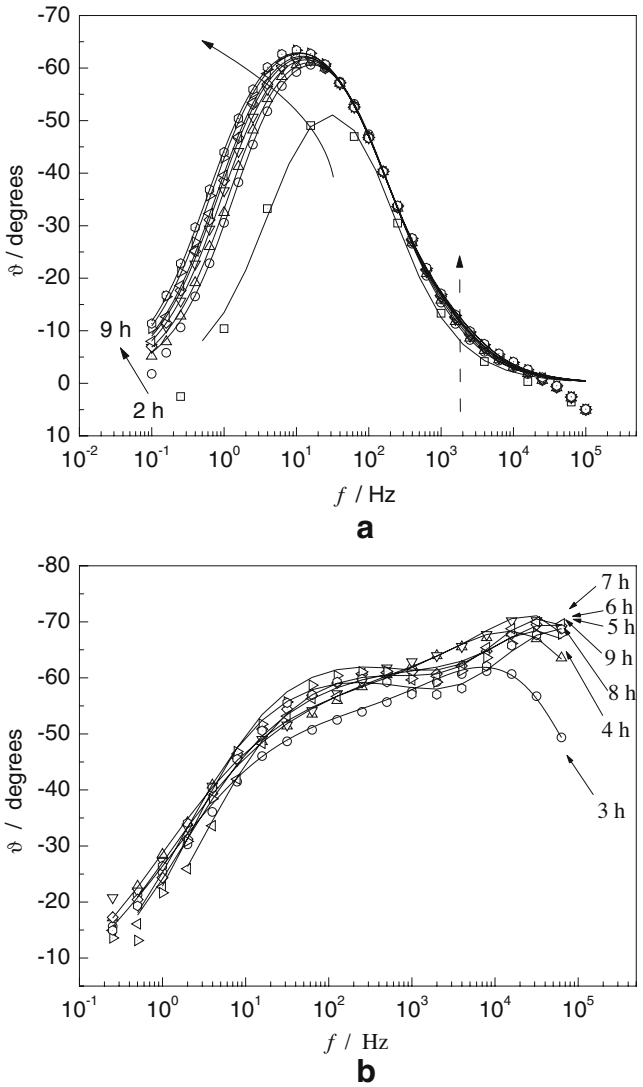

Fig. 10 Bode diagrams for 1018 carbon steel in **a** 3% NaCl and **b** 3% NaCl + diesel solutions with inhibitor HEI-18

magnitude is one order of magnitude higher than that obtained with the uninhibited solutions (Fig. 6a). Calculated efficiencies for HEI-18 and HEI-18I inhibitors by using Eq. 2 after 9 h of immersion time were 90.04%, whereas for inhibitor HEI-12, it was 90.00%, practically the same.

Nyquist impedance spectra, for the 3% NaCl + diesel after addition of inhibitors at different exposure times are shown in Fig. 9a–c, respectively. The magnitude of the impedance increases continuously with time for both solutions. All experimental spectra have a depressed

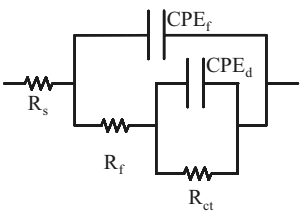

Fig. 11 Equivalent circuit used to represent the impedance results for inhibited solutions

Table 5 Circuit parameters for sample 1018 carbon steel in 3% NaCl with inhibitor HEI-18

t (h)	R_s (Ω)	CPE_f		R_f (Ω)	CPE_d		R_{ct} (Ω)
		Y_f (Ω^{-1} s^n) $\times 10^{-3}$	n		Y_{dl} (Ω^{-1} s^n) $\times 10^{-3}$	n	
2	0.55	–	–	–	4.99	0.809	13.08
3	0.58	1.06	0.808	0.94	2.80	0.790	57.68
4	0.66	1.07	0.816	0.64	3.27	0.783	68.92
5	0.58	1.06	0.815	0.58	3.19	0.781	80.66
6	0.58	1.07	0.812	0.60	3.08	0.778	93.49
7	0.59	1.09	0.809	0.66	2.92	0.779	107.2
8	0.60	1.48	0.812	0.74	2.89	0.777	119.6
9	0.60	1.59	0.810	0.79	2.86	0.776	130.00

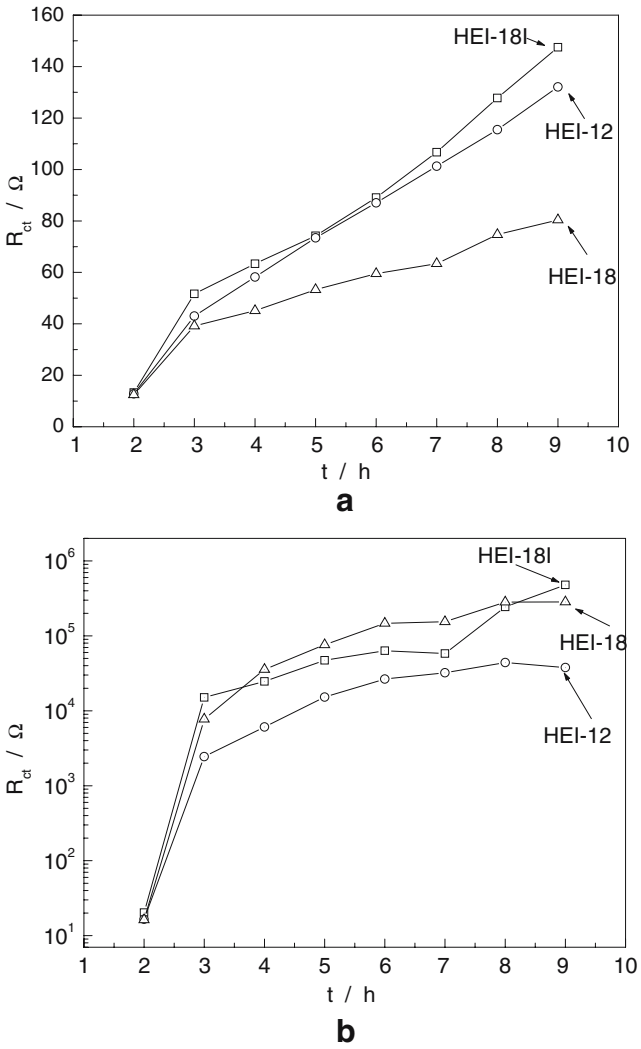

Fig. 12 Change in the charge transfer resistance value, R_{ct}, for the different imidazolines in **a** 3% NaCl and **b** 3% NaCl + diesel solutions

semicircular shape in the complex impedance plane, with the center under the real axis. The magnitude of the impedance with hydroxyethyl imidazolines is up to 5 orders of magnitude higher than the impedance obtained for the blank solution (Fig. 6b), except for inhibitor HEI-12, with an impedance magnitude four orders of magnitude higher than the corresponding uninhibited solution. This is expected as the inhibitor used was oil soluble, and thus, the inhibitor would be transported to the surface when the oily part was present. The calculated efficiencies in all cases this time was higher than 99% for all inhibitors. Thus, it seems that the presence of the oily phase has an effect of co-adsorption of the inhibitor on the substrate, which improved the performance of the inhibitor.

Figure 10 shows the corresponding bode plot for the same experimental data in the log f vs θ format for inhibited 3% NaCl solutions without and with diesel, respectively, for inhibitor HEI-18. This figure clearly shows the presence of a single phase shift at 100 Hz, which is shifting to lower frequencies as time elapses. There is no evidence of the formation of a protective $FeCO_3$ film because there is only one capacitive loop in the EIS Nyquist plots [21]. One would expect to see a new phase angle shift at higher frequency range and a continuous increase in the phase angle shift with time during film formation. However, when the oily phase is present in the solution, significant changes are noted. As shown in Fig. 10b, there is a new phase angle shift at higher frequencies than 100 Hz, and the position of the peak at high frequencies is shifted towards frequencies as the immersion time increases. Consistent with other authors [8, 19], the high frequency loop can be ascribed to the inhibitor film because its small time constant causes a phase shift in the high-frequency limit. According to these authors, the presence of long hydrocarbon chains in the structure of the imidazolines is responsible for their capacity of forming protective barriers against aggressive ions from the bulk solution.

Different equivalent circuits have been established to interpret the impedance behavior of coated electrodes with

Table 6 Circuit parameters for 1018 carbon steel in 3% NaCl + diesel with inhibitor HEI-18

t (h)	R_s (Ω)	CPE_f		R_f (Ω)	CPE_d		R_{ct} (Ω) $\times 10^4$
		Y_f (Ω^{-1} s^n) x 10^{-6}	n		Y_{dl} (Ω^{-1} s^n) x 10^{-5}	n	
2							
3	1.83	2.493	0.93	36.97	4.043	0.56	0.849
4	1.61	3.439	0.88	219.5	2.380	0.56	0.835
5	1.77	1.263	0.93	147.4	1.385	0.63	1.786
6	2.27	0.719	0.98	84.09	1.220	0.65	1.935
7	1.86	1.256	0.91	413.4	0.604	0.70	1.665
8	2.08	1.360	0.89	877.9	0.460	0.71	2.212
9	1.49	1.636	0.87	3231	0.329	0.73	3.340

film inhibitors (imidazolines) [1–3, 5–8]. The equivalent circuit shown in Fig. 11 was used to describe the electrochemical process in the presence of the inhibitor for both testing solutions. For metal electrodes without coating, the diameter of the high frequency semicircle is treated as the charge transfer resistance R_{ct}. However, for coated electrodes, the high frequency capacitive loop is related to the barrier and properties of the film. In the equivalent circuit in Fig. 11, R_s, R_{ct}, and CPE_d have the same physical meanings as in Fig. 7, CPE_f represents the capacitance of the film, and R_f represents the resistance of the film, which reflects the protective properties of the film. The fitting parameters obtained using the electrical circuit shown in Fig. 11 are presented in Tables 5 and 6 as an example for inhibitor HEI-18 without and with the addition of diesel. The fitting curves are presented in Figs. 8 and 9 as solid lines for each spectrum, observing an optimum fit with the model for all experimental data with en error of 3% in all cases. Apparently, we have two time constants, which is approximately true. Actually, we have one time constant and one distribution of time constant because we have a constant phase element.

Figure 12 shows the calculated charge transfer resistance for these solutions. From Tables 5 and 6 and Fig. 12, it can be seen that when diesel is present, both R_f and R_{ct} had the maximum values for inhibitor HEI-18I, which provided the highest corrosion protection efficiency. Also, the calculated proportional factor Y_{dl} of CPE for the 3% NaCl + Diesel solution decreases with time, and its film resistance values are similar to the charge transfer resistance, which could be related to the formation of a protective $FeCO_3$ layer. Even more, the charge transfer resistance value, R_{ct}, for the 3% NaCl solution increased with time, whereas both the R_{ct} and R_f values for the 3% NaCl + diesel solution reached a quasi stable value after a few hours of immersion, confirming that the film formation is faster with diesel. According to Cottis [22], the R_{ct} values obtained from Nyquist plots like the ones shown on Figs. 8 and 9 are equivalent to the R_p values obtained from the linear polarization resistance tests shown on Fig. 5. This is done by subtracting the solution resistance from the total impedance in the Nyquist spectra. We can see that there exists a good correlation between the R_{ct} shown on Tables 5 and 6 and the R_p values shown on Fig. 5. For instance, R_{ct} values exhibited on Table 5 for 3% NaCl solution without diesel using inhibitor HEI-18 lie between 13.08 and 130 ohms, very close to the R_p values for the same solution as shown on Fig. 5c. On the other hand, the R_{ct} values for the 3% NaCl + diesel solution shown on Table 6 lie between 849 and 3,340 ohms, slightly lower than the R_p values exhibited by Fig. 5c. According to Ramachandran [7], the formed film by the presence of long hydrocarbon chains in the structure of the imidazolines acts as a protective barrier against aggressive ions from he bulk solution.

Conclusions

1. In 3% NaCl solutions, the corrosion rate is decreased with the addition of modified hydroxyethyl imidazolines inhibitors, but the time to reach a steady state was significantly shortened when diesel is simultaneously added .
2. The relative efficiencies of the three compounds studied in deaerated 3% NaCl + diesel at 50 °C is found to be in the following order: HEI-18 > HEI-18I≈HEI-12. The efficiencies were higher when diesel was present than when it was absent.
3. The reason seems to be that the inhibitors are not soluble in water but oil soluble, so when diesel is present, inhibitors are easily transported towards the metal surface to be adsorbed and form a protective film.

References

1. Kermani MB, Morshed A (2003) Corrosion 59:659
2. Jovancicevic V, Ramachandran S, Prince P (1999) Corrosion 55:449
3. Ramachandran S, Jovancicevic V (1999) Corrosion 55:259
4. Xueyuan Z (2001) Corros Sci 43:1417
5. Bentiss F, Lagrenee M, Traisnel M, Hornez JC (1999) Corros Sci 41:789
6. Bentiss F, Traisnel M, Lagrenee M (2001) J Appl Electrochem 31:449
7. Villamisar W, Casales M, Gonzalez-Rodriguez JG, Martinez L (2007) J Solid State Electrochem 11:619
8. Ramachandran S, Tsai M, Blanco M, Chen H, Tang WA, Godard III (1996) Langmuir 12:6419
9. Wang D, Li S, Ying M, Wang M, Xiao Z, Chen Z (1999) Corros Sci 41:1911
10. Cruz J, Martinez-Aguilera LMR, Salcedo R, Castro M (2001) Int J Quant Chem 85:546
11. Cruz J, Martinez R, Genesca J, Garcia-Ochoa E (2004) J Electroan Chem 566:111
12. Rodriguez-Valdez LM, Martinez-Villafañe A, Golztman-Mitnik D (2004) Theochem 681:83
13. Rodriguez-Valdez LM, Martinez-Villafañe A, Golztman-Mitnik D (2005) 713:65
14. Bilkova K, Hackerman N, Bartos M (2002) Proceedings of NACE Corrosion/2002, NACE Denver, CO, paper No. 2284
15. Quiroga-Becerra H, Retamoso C, MacDonald D (2000) Corros Sci 42:561
16. ASTM G 5-94, "Standard reference test method for making potentiostatic and potentiodynamic anodic polarization measurements", ASTM International
17. Thompson NG, Payer J H (1998) « DC Electrochemical Test Methods » Corrosion testing made easy series, series. BC Syrret (ed), National Association of Corrosion Engineers, Houston, TX, U S A
18. Macdonald JR (1987) J Electroanal Chem 223:25
19. De Moraes FD, Shadley JR, Chen J, Rybicki E (2000) Proceedings of the NACE Corrosion/2000, NACE 2000, Orlando FL Paper No. 30
20. Walter GW (1989) Corros Sci 26:681
21. Mansfield F (1990) Electrochim Acta 35:1533
22. Cottis R, Turgoose S (1999) « Electrochemical Impedance and Noise », Corrosion testing made easy series, series, BC Syrret (ed), National Association of Corrosion Engineers, Manchester, U K